Electronic Supplementary Material (ESI) for Nanoscale.

Metadynamics simulations for the investigation of drug loading on functionalized inorganic nanoparticles

Stefano Motta,[a] Paulo Siani,[b] Edoardo Donadoni,[b] Giulia Frigerio,[b] Laura Bonati,[a] and Cristiana Di Valentin*[b,c]

[a] *Dipartimento di Scienze dell'Ambiente e del Territorio, Università di Milano Bicocca, Piazza della Scienza 1, 20126 Milano, Italy.*
[b] *Dipartimento di Scienza dei Materiali, Università di Milano Bicocca, via R. Cozzi 55, 20125 Milano, Italy.*
[c] *BioNanoMedicine Center NANOMIB, University of Milano-Bicocca, Italy.*
**Corresponding author: cristiana.divalentin@unimib.it*

Electronic Supplementary Information

Table S1: Parameters of the different MetaD simulations

Biased CV	MetaD approach	Deposition rate (ps)	Hills Height (kj/mol)	Hills Width (kj/mol)	Simulation length (μs)
d	St	3	0.5	0.04 Å	1.6
d,Φ	St	1	0.5	0.05 Å, 0.06 rad	1.5
d,C	St	1	0.5	0.05 Å, 0.01	3.4
d	WT	3	0.5	0.04 Å	2.0
d,C	WT	1	0.5	0.05 Å, 0.01	1.5

Fig. S1: DOX atoms used for the distance calculation for SOM training.

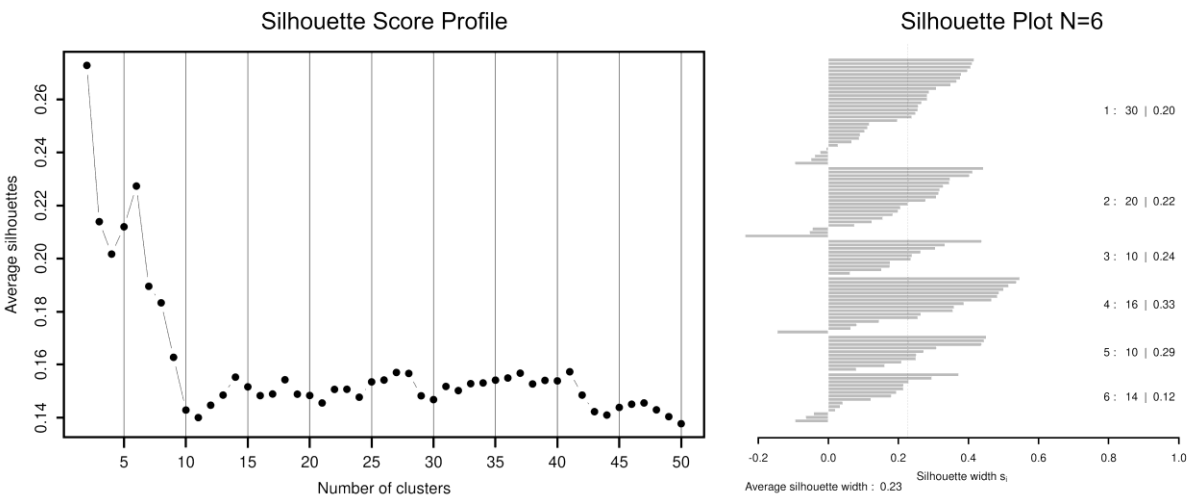

Fig. S2: Choice of the best number of clusters. The average silhouette width is reported against the number of clusters (left). For the chosen number of clusters (right) the detailed silhouette profile is reported.

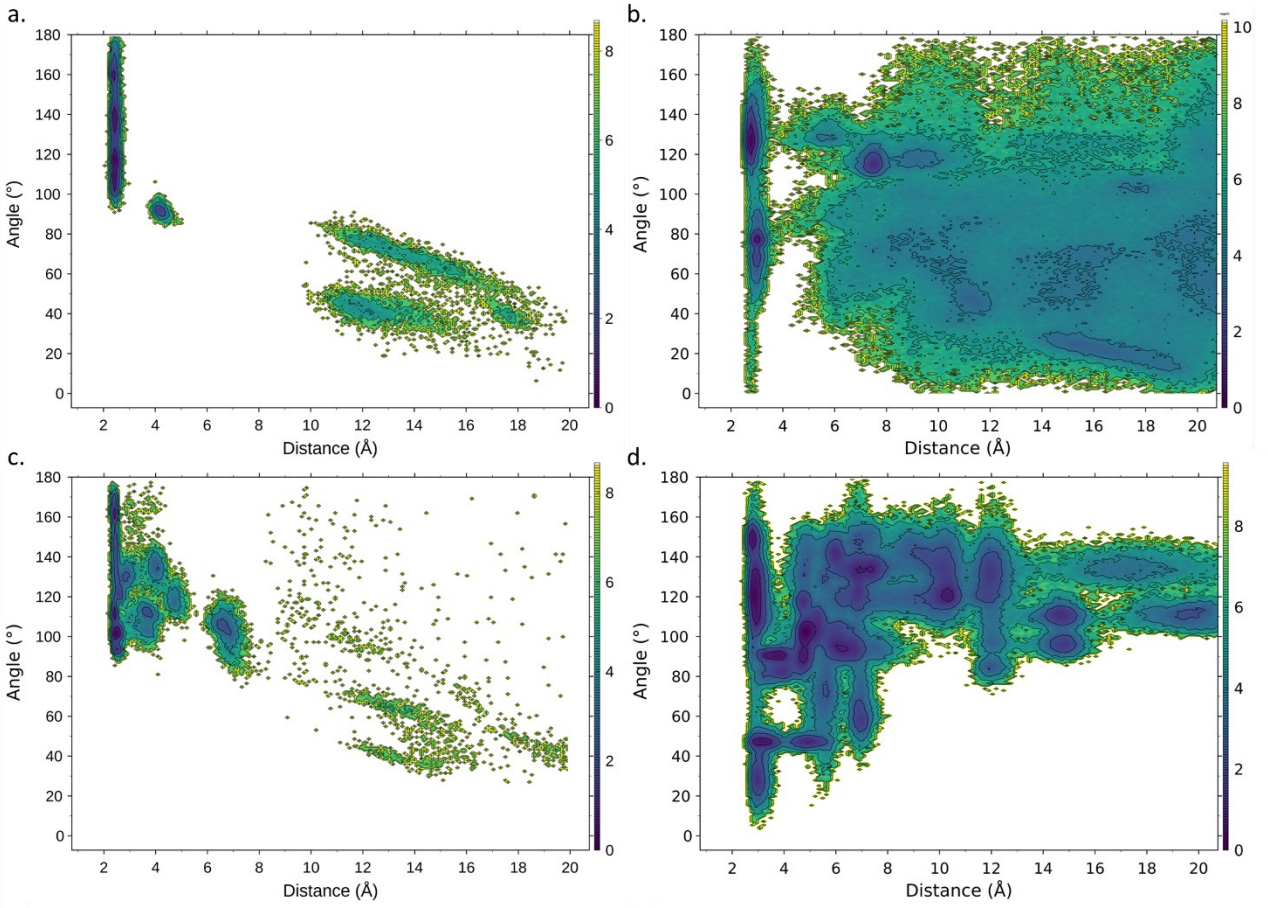

Fig. S3: Relevant DOX binding states identified on the probability density map along two selected variables. Variables are the distance between the DOX nitrogen atom and the closest NP atom; the angle formed between the center of the NP, the DOX nitrogen atom and the carbon on the opposite side of the anthraquinone ring. Results are shown for a) Brandt et al. 2015 TiO_2 parameters with fully protonated TETTs; b) Rouse et al. 2021 TiO_2 parameters with fully protonated TETTs; c) Brandt et al. 2015 TiO_2 parameters with mono deprotonated TETTs; d) Rouse et al. 2021 TiO_2 parameters with mono deprotonated TETTs.

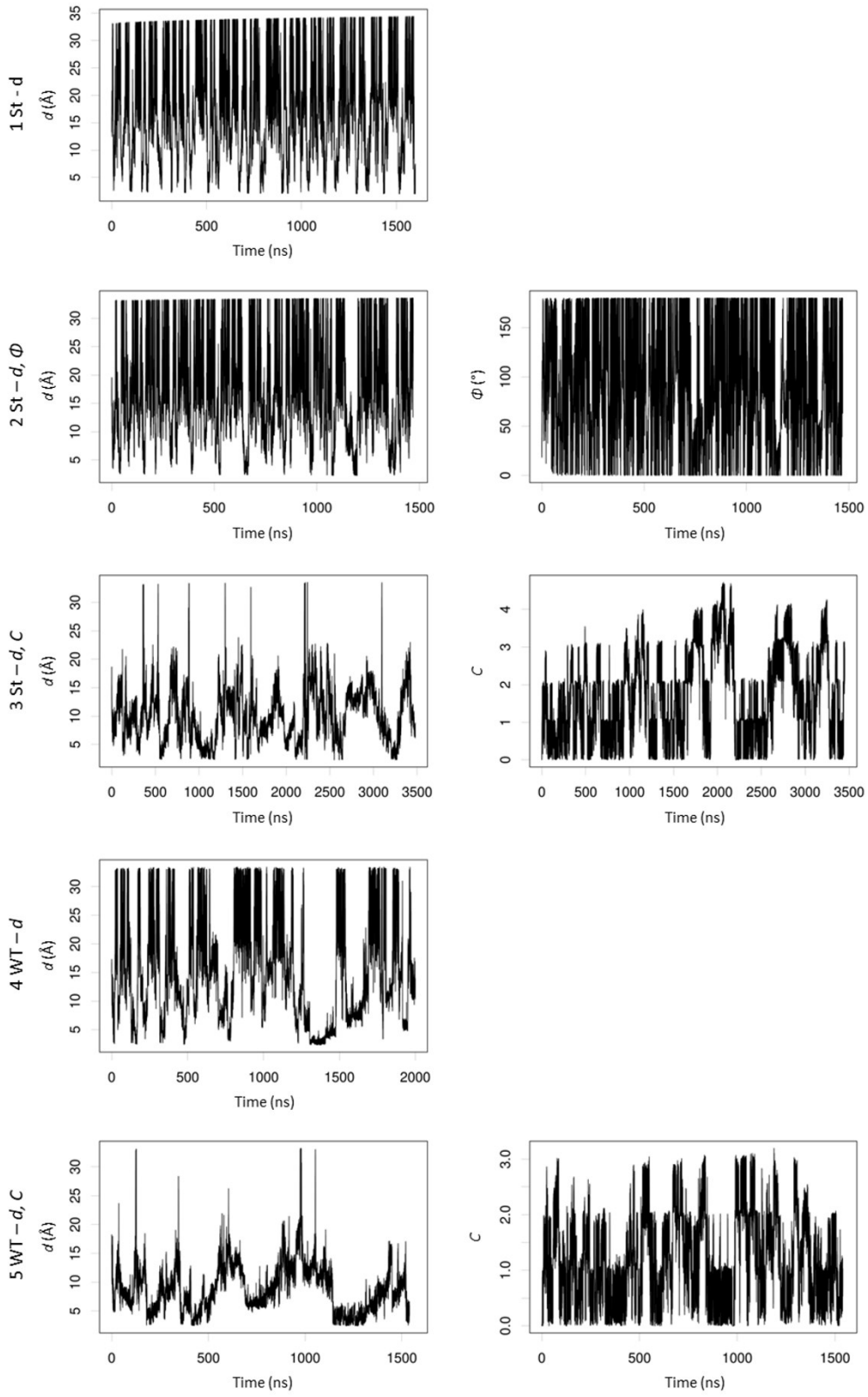

Fig. S4: Monitor of the CVs during the MetaD simulations in slightly acidic conditions.

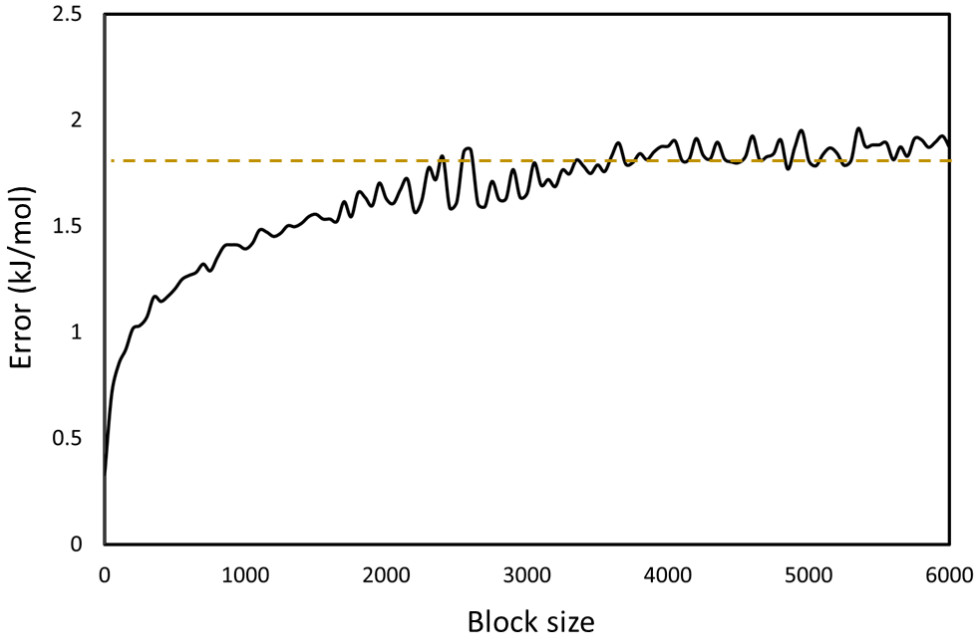

Fig. S5: Block analysis of a St-MetaD simulation using *d* as CV.

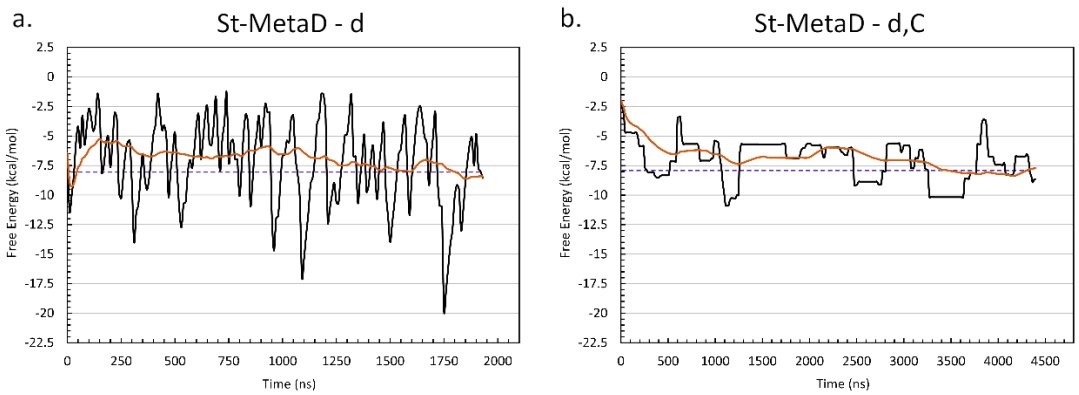

Fig. S6: Convergency plot of the binding free energy difference between the bound and unbound states for the different simulations: a) St.MetaD biasing only d; b) St-MetaD biasing d and C; The value of the free energy difference as the simulation evolves is plotted as black lines, the running averages as orange lines and the final averaged value as purple dashed lines.

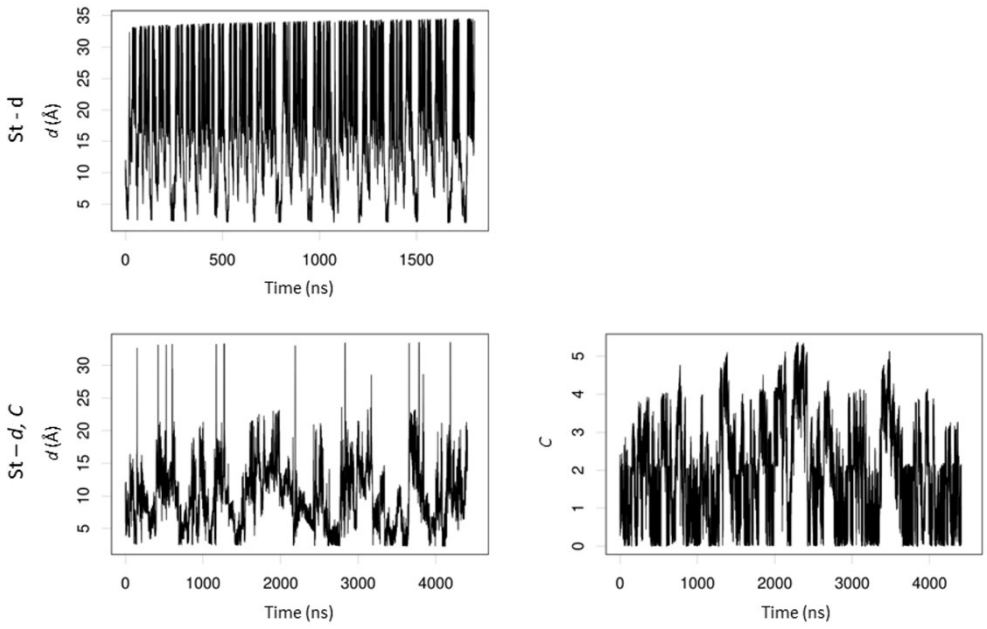

Fig. S7: Monitor of the CVs during the MetaD simulations at neutral pH conditions.

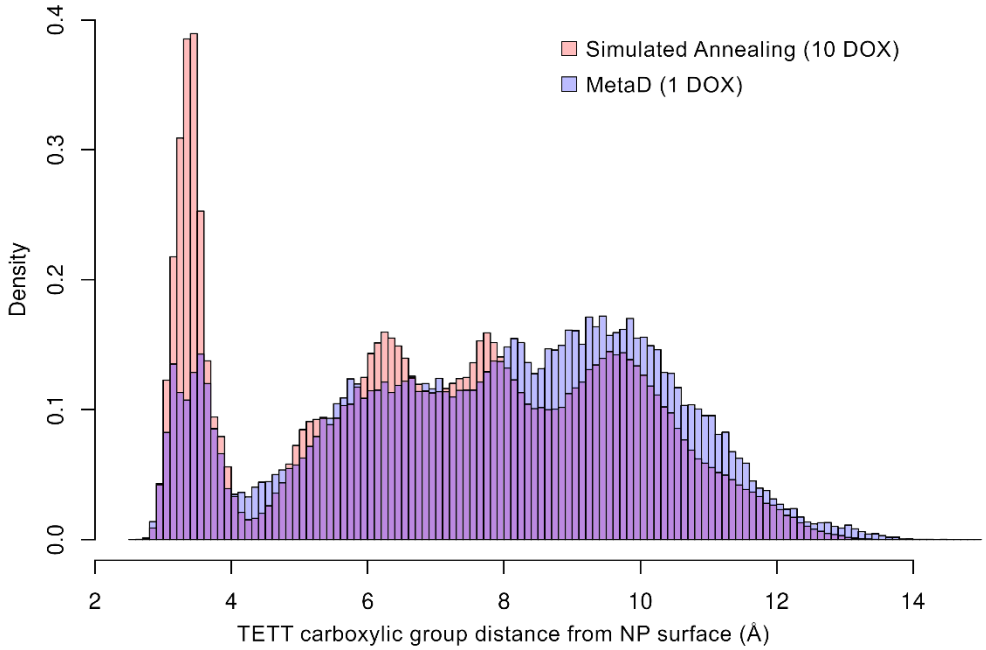

Fig. S8: Monitor of the distance from the NP surface of the two carboxylic groups that lie at the furthest extremity of the TETT chains. Histogram represents the probability of finding the carboxylic group at a certain distance from the NP surface during simulated annealing simulations with 10 DOX (red) and St-MetaD simulation biasing only *d* with a single DOX. Both simulations were performed with one carboxylic group deprotonated for each TETT chain (slight acidic conditions).

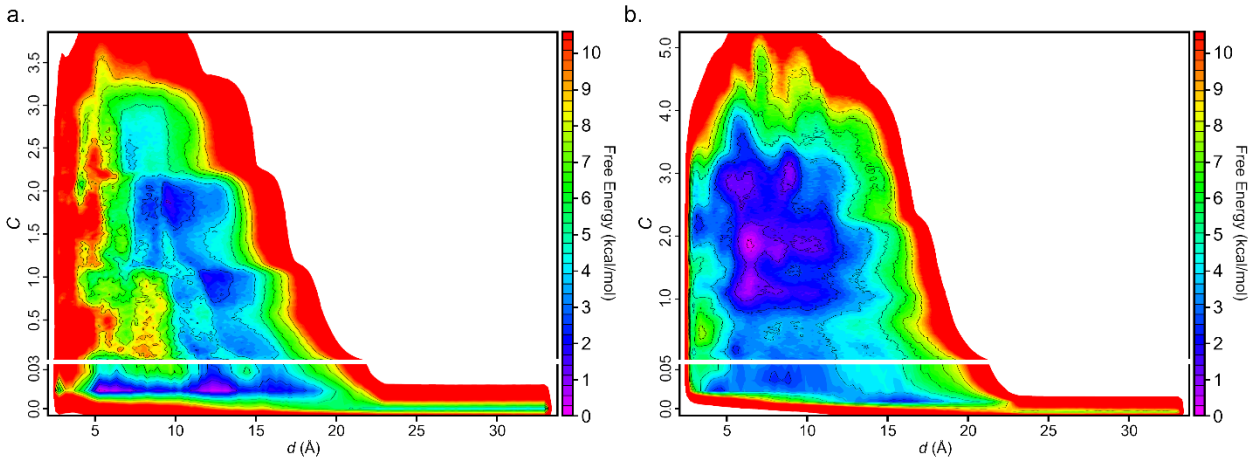

Fig. S9: Free-energy surface for the simulation biasing d and C in a) acidic pH; b) neutral pH. In the graphs the y-scale is modified to enlarge the region around values of C near 0.

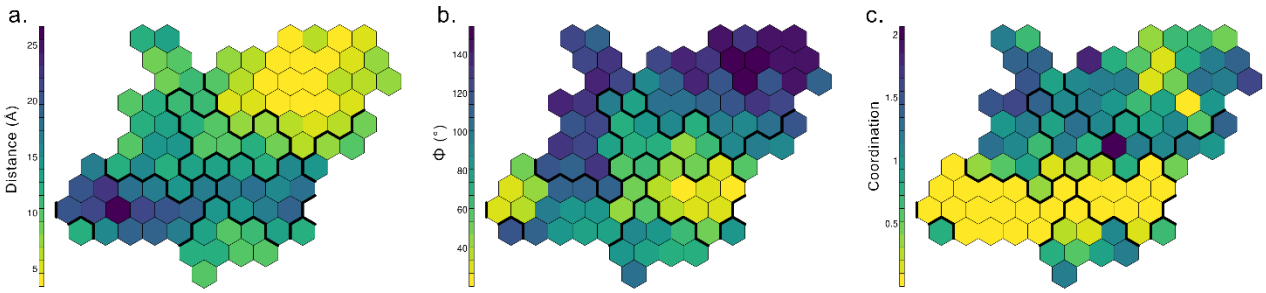

Fig. S10: Average values of the a) *d* CV; b) *Φ* CV; c) *C* CV computed per neurons.